



Catalytic hydrazine disproportionation mediated by a thiolate-bridged VFe complex

Journal:	<i>ChemComm</i>
Manuscript ID	CC-COM-01-2019-000345.R1
Article Type:	Communication

SCHOLARONE™
Manuscripts

Catalytic hydrazine disproportionation mediated by a thiolate-bridged VFe complex

Nina X. Gu,^a Gaël Ung,^b and Jonas C. Peters^{*a}

Received 00th January 20xx,
Accepted 00th January 20xx

DOI: 10.1039/x0xx00000x

www.rsc.org/

A heterobimetallic VFe complex is demonstrated to catalyse hydrazine disproportionation with yields of up to 1073 equivalents of NH₃ per catalyst, comparable to the highest turnover known for any molecular catalyst. Notably, the heterobimetallic complex is appreciably more active than monometallic analogues of the V and Fe sites, suggesting that bimetallic cooperativity may facilitate the observed catalysis.

Despite structural similarities between the MoFe and VFe nitrogenase cofactors,¹ these variants demonstrate variable efficiencies for nitrogen fixation,² and it is unknown how the distinct metal compositions of the cofactors influence catalytic performance, and the mechanistic pathways that are viable. Similarly, questions remain regarding which metal site(s) are active toward nitrogen fixation at the VFe cofactor,³ and whether bimetallic cooperativity between V and Fe sites may play a role. Synthetic V⁴ and Fe⁵ complexes are now known that catalyse molecular N₂ reduction to NH₃ (or hydrazine). It remains of interest to study the reactivity of bimetallic MFe (M= Mo, V, Fe) complexes toward N₂ and other nitrogenous substrates to canvas accessible chemistry on such systems.

N₂ binding to heterobimetallic VFe complexes has not been previously demonstrated, and relatedly, there are as yet no examples of heterobimetallic VFe-based molecular N₂ fixation catalysts. However, VFe complexes are known to generate ammonia via reduction of hydrazine (N₂H₄ + 2 H⁺ + 2 e⁻ → 2 NH₃),⁶ which is both a detectable product of biological nitrogen fixation,⁷ as well as a substrate for some nitrogenases.⁸ Alternatively, the 2 H⁺/2 e⁻ employed in the reduction of hydrazine may be derived from hydrazine itself via a disproportionation pathway, coupling the reduction of N₂H₄ to NH₃ to the oxidation of N₂H₄ to N₂ (3 N₂H₄ → 4 NH₃ + N₂).^{9,10}

Whether N₂H₄ is an essential intermediate of biological nitrogen fixation is not known. Nonetheless, one possible pathway to catalyse nitrogen fixation to ammonia is the selective reduction N₂ to N₂H₄, which has been demonstrated both stoichiometrically¹¹ and catalytically in molecular Fe systems,^{5d} followed by subsequent hydrazine disproportionation.

Herein, we synthesize a thiolate-supported vanadium-iron complex, with N₂ and hydride ligands bound to the Fe centre, and demonstrate that it is an active catalyst for the disproportionation of hydrazine under ambient conditions, achieving yields of up to 1073 equivalents of NH₃ per VFe complex. In comparison to the bimetallic complex, monometallic analogues of the individual V and Fe centres display attenuated catalytic activity, which suggests a cooperative bimetallic mechanism may be operative in the disproportionation reaction.

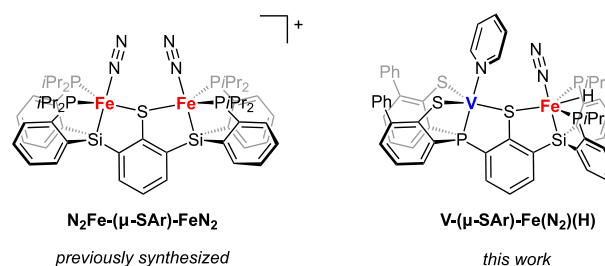


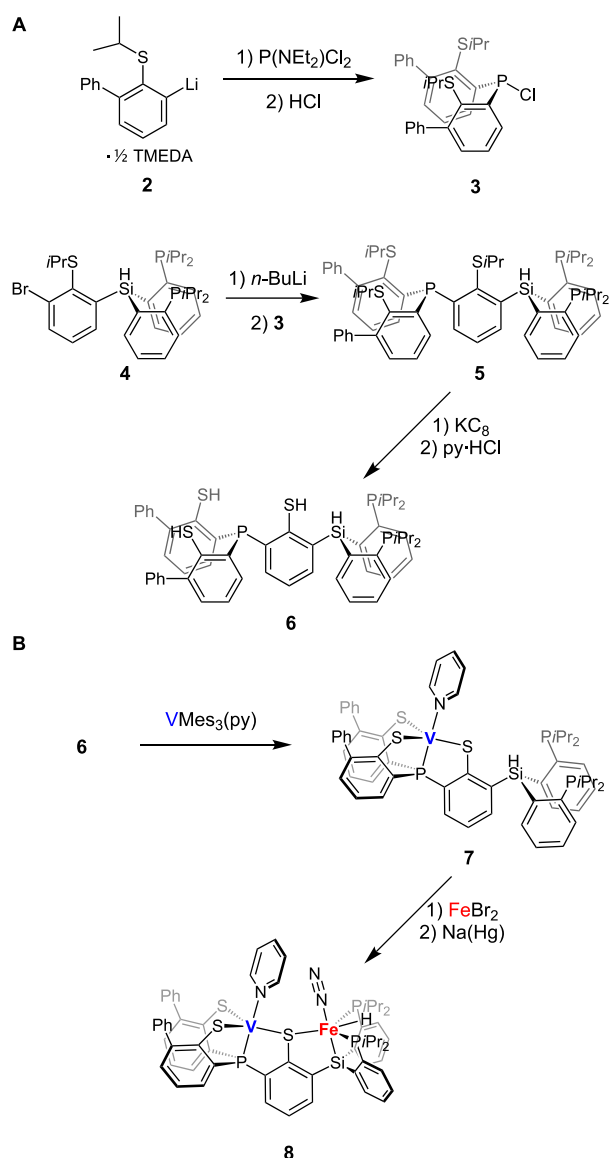
Figure 1. Thiolate-bridged bimetallic complexes N₂Fe-(μ-SAr)-Fe(N₂) (**1**) and V-(μ-SAr)-Fe(N₂)(H) (**8**)

To template the target VFe complex, we modified the binucleating ligand used to support the thiolate-bridged diiron complex N₂Fe-(μ-SAr)-Fe(N₂) (**1**), previously reported by our lab (Fig. 1),¹⁰ to incorporate a (polythiolate)phosphine fragment to coordinate V.¹² Treatment of the thioether-substituted aryllithium **2**¹³ with dichloro(diethylamino) phosphine (0.5 equivalent), followed by addition of HCl, yields the thioether-substituted diaryl(chloro)phosphine (**3**, Scheme 1a). Lithium-halogen exchange of (diphosphino)thioether-functionalized triarylsilane **4** and subsequent treatment with **3** yields the thioether-protected ligand precursor **5**. Reductive cleavage of

^a Division of Chemistry and Chemical Engineering, California Institute of Technology, Pasadena, California, 91125, USA. E-mail: jpeters@caltech.edu

^b Department of Chemistry, University of Connecticut, Storrs, Connecticut, 06269, USA.

Electronic Supplementary Information (ESI) available: Synthetic details, crystal structure data, and spectroscopic data, see DOI: 10.1039/x0xx00000x



Scheme 1. (a) Synthesis of ligand **6** and (b) metalation of complexes **7** and **8**.

the *S*-*i*Pr groups with excess KC_8 and subsequent protonation yields the thiol-functionalized ligand **6**.

Treatment of **6** with $\text{VMes}_3(\text{py})$ ($\text{Mes} = 2,4,6\text{-Me}_3\text{C}_6\text{H}_2$, $\text{py} = \text{NC}_5\text{H}_5$) generates $\text{V}(\text{SAr})$ (**7**, Scheme 1b). Compound **7** is a yellow-orange solid and has a spin state of $S = 1$ at 25°C . Stirring **7** with iron dibromide, followed by reduction with $\text{Na}(\text{Hg})$ amalgam (2.1 equiv. Na) under an N_2 atmosphere yields $\text{V}(\mu\text{-SAr})\text{-Fe}(\text{N}_2)(\text{H})$ (**8**) in moderate yields, whereby reduction promotes the Fe-centred Si-H bond cleavage and N_2 coordination. Compound **8** has a solution magnetic moment of $3.1\mu_{\text{B}}$ (25°C), consistent with an overall $S = 1$ species.

Despite repeated attempts, only moderate-quality crystallographic data could be obtained on compound **8**. Nonetheless, the XRD data support the structural assignment of **8** (Fig. 2). The Fe-bound hydride could not be located in the XRD data of **8**, but the large $\angle\text{P-Fe-P}$ angle ($153.0(6)^\circ$) suggests it is positioned trans to the thiolate. The IR spectrum of **8** reveals an Fe-H stretch at 1898 cm^{-1} , which corroborates the presence of

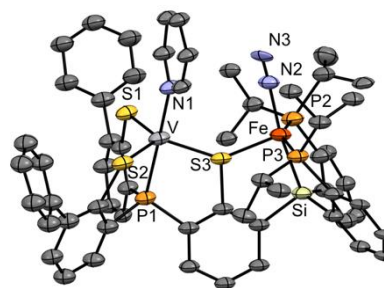


Figure 2. X-ray structure of **8**. Hydrogen atoms and solvent molecules are omitted for clarity. Ellipsoids are depicted at 50% probability.

the hydride ligand. Additionally, treatment of **8** with one equivalent of $[\text{H}(\text{OEt}_2)][\text{Bar}^{\text{F}_4}]$ results in the protonation of the hydride ligand to form H_2 . The N_2 stretch is observed at 2054 cm^{-1} , similar to that of a structurally related diamagnetic ferrous species, $(\text{SiPr}_2\text{S}^{\text{Ad}})\text{Fe}(\text{H})(\text{N}_2)$ (**9**, 2055 cm^{-1} , Fig. 3).¹⁴ This comparison is consistent with a description for **8** as a $\text{V}(\text{III})/\text{Fe}(\text{II})$ species. In an alternate oxidation state assignment, if the bridging thiolate is described as an L-type ligand to V and an X-type ligand to Fe, compound **8** can instead be considered a $\text{V}(\text{II})/\text{Fe}(\text{III})$ species. However, the IR spectrum of a related ferric hydride, $(\text{SiPr}_2\text{S})\text{Fe}(\text{H})(\text{N}_2)$ (**10**),¹³ exhibits a significantly less activated N_2 stretch of 2123 cm^{-1} .¹⁵ Thus, we favour the description of **8** as bearing an $S = 1$ $\text{V}(\text{III})$ centre and an $S = 0$ $\text{Fe}(\text{II})$ centre. Of note, a related thiolate-bound $\text{V}(\text{III})$ species (**11**) has a spin state of $S = 1$ at 25°C .

Complex **8** is an active catalyst for the disproportionation of hydrazine ($3\text{ N}_2\text{H}_4 \rightarrow 4\text{ NH}_3 + \text{N}_2$).¹⁶ Treatment of **8** with 50 equivalents of hydrazine results in the detection of NH_3 after 2 hours (Table 1), with higher yields of ammonia using Et_2O (10 equiv. $\text{NH}_3/\mathbf{8}$, 16%, entry a) as a solvent as compared to THF (5 equiv. $\text{NH}_3/\mathbf{8}$, 7%, entry b). Employing Et_2O as the solvent, 46 equivalents of NH_3 per VFe complex were detected after 12 hours of reaction time (69%, entry c), and 60 equivalents of NH_3 were produced after 24 hours of reaction time (89%, entry d). At higher substrate loading (100 equiv. $\text{N}_2\text{H}_4/\mathbf{8}$), 89 equivalents of NH_3 were produced after 24 h (67%, entry e), and 113 equivalents after 48 h (85%, entry f). Addition of elemental Hg or PPh_3 did not affect catalysis.¹⁷

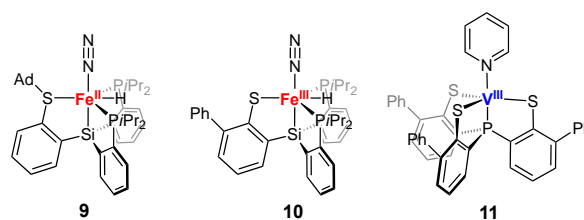


Figure 3. Monometallic complexes **9-11**. Ad = adamantyl

There are no previously reported examples of vanadium complexes that facilitate the catalytic disproportionation of N_2H_4 , although V complexes have been demonstrated to catalyse hydrazine reduction^{12d} and the disproportionation of substituted hydrazines.¹⁸ When considering Fe-only catalysts, diiron **1** bears the highest previously reported turnover number; in the presence of one equivalent of co-acid, treatment of **1** with 50 equivalents N_2H_4 yields 29 equivalents of NH_3 (44% yield).¹⁰

Table 1. N₂H₄ disproportionation catalysed by compound **8**

$3 \text{ N}_2\text{H}_4 \xrightarrow[\text{Et}_2\text{O}, 25^\circ\text{C}]{\text{compound } \mathbf{8}} 4 \text{ NH}_3 + \text{N}_2$				
Entry	Time	N ₂ H ₄ (equiv./ 8)	NH ₃ (equiv./ 8)	NH ₃ (%)
<i>a</i>	2 h	50	10(1)	16
<i>b</i> ¹	2 h	50	5(1)	7
<i>c</i>	12 h	50	46(7)	69
<i>d</i>	24 h	50	60(4)	89
<i>e</i>	24 h	100	89(12)	67
<i>f</i>	48 h	100	113(16)	85
<i>g</i>	17 d	1440	1073(84)	56

Catalytic runs are performed at catalyst concentrations of 1 mM unless otherwise noted. Yields are an average of 2 runs; the spread between the two runs is shown in parentheses as a std deviation for N = 2, and values for all individual runs are presented in the Supporting Information. ¹Entry b was carried out with THF as the solvent. ²Entry g was carried out with a catalyst concentration of 0.1 mM.

To the best of our knowledge, the most active molecular hydrazine disproportionation catalyst with respect to turnover number is a dimolybdenum complex, which generated 1232 equivalents of NH₃ per complex (1440 equivalents of N₂H₄, 64% yield) over 17 days.^{9g,h} For direct comparison, treatment of **8** with 1440 equivalents of N₂H₄ yielded 1073 equivalents of ammonia (56%) over the same time period (Table 1, entry g), demonstrating their similar activities.

Table 2. N₂H₄ disproportionation catalysed by compounds **9** and **11**.

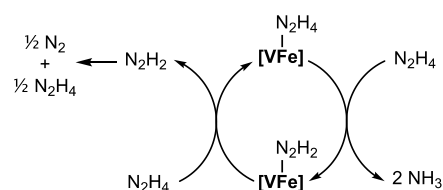
$3 \text{ N}_2\text{H}_4 \xrightarrow[\text{THF}, 2 \text{ h}, 25^\circ\text{C}]{2\% \text{ catalyst}} 4 \text{ NH}_3 + \text{N}_2$		
Entry	Catalyst	NH ₃ (equiv./cat.)
<i>h</i>	9	0.4(0.2)
<i>i</i>	11	0.2(0.1)
<i>j</i> ¹	9 + 11	1.0(0.2)

Catalytic runs are performed at catalyst concentrations of 1 mM unless otherwise noted. Yields are an average of 2 runs; the spread between the two runs is shown in parentheses as a std deviation for N = 2, and values for all individual runs are presented in the Supporting Information. ¹[**9**] = [**11**] = 1 mM.

The catalytic activities of the monometallic Fe and V analogues (**9** and **11**) were assayed to compare their respective activities with that of bimetallic **8**. Upon treatment of 50 equiv of hydrazine in THF (Table 2),¹⁹ complexes **9** (0.4 equiv/**9**, entry h) and **11** (0.2 equiv/**11**, entry i) yielded far less NH₃ than **8** (5 equiv/**8**, Table 1, entry b) after 2 hours. Additionally, an equimolar mixture of **9** and **11** yielded 1.0 equiv of NH₃/**9** after 2 hours (Table 2, entry j), which is comparable to the sum of their independent yields in entries h and i. While we do not know all the factors at play, the poorer activity of the equimolar mixture of **9** and **11** compared to that of **8** suggests that arrangement of the Fe and V centres in a binucleating scaffold may enhance the activity for ammonia formation.

Employing the method of initial rates, a pseudo-zero order dependence on N₂H₄ is observed at high substrate loadings (ca. 50 equiv. N₂H₄) in THF,²⁰ which is due to saturation kinetics and

is relevant to the catalysis at early timepoints. Probing kinetics at lower substrate loadings (ca. 10 equiv. of N₂H₄), a first order dependence on N₂H₄ is determined, which is the regime that the catalyst operates under at late timepoints when most of the substrate has been consumed. Additionally, a first order dependence on **8** is measured, which is consistent with a unimolecular pathway with respect to the VFe catalyst, as depicted in Figure 4. However, an on-path step involving two VFe species cannot be ruled out. Here, a formal dihydrogen transfer between two hydrazine species yields two equivalents of ammonia and one equivalent of diazene, which can undergo thermal decomposition upon release,²¹ followed by N₂H₄ binding to close the catalytic cycle. The dominant decomposition pathway for diazene yields half an equivalent of dinitrogen and half an equivalent hydrazine. Additionally, it has been proposed as an intermediate in other hydrazine disproportionation systems.^{9e,i}

**Figure 4.** Proposed catalytic cycle for hydrazine disproportionation catalysed by **8**.

Drawing inspiration from the VFe cofactor, we have synthesized an N₂-bound VFe complex with supporting thiolate, phosphine, and silyl donors, and demonstrated that it is a highly active catalyst for hydrazine disproportionation with respect to turnover number, as active as any known. Whereas there are no known V catalysts for N₂H₄ disproportionation, there are several less active Fe complexes that also catalyse this transformation.⁹ It is unclear whether both metal centres are synergistically participating in the key bond-breaking and -forming steps, but assuming that the monometallic complexes **9** and **11** are representative models for the catalytic activities of the Fe and V centres of **8**, the much poorer activity of the vanadium and iron monometallic species compared to the activity of **8** indicates that arranging the two metal centres within the bimetallic scaffold described promotes hydrazine disproportionation catalysis.

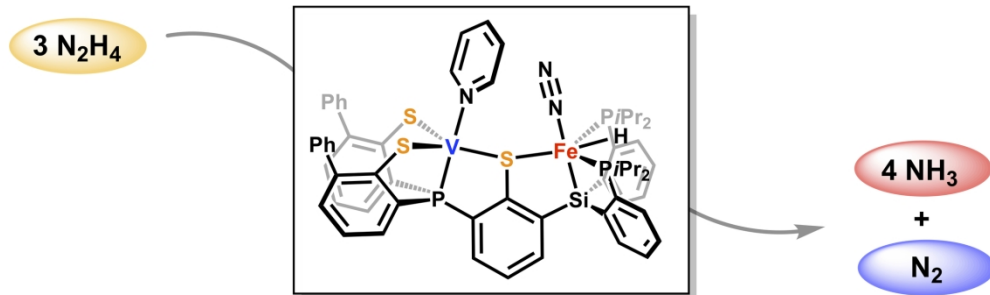
This work was supported by the Department of Energy (DOE-0235032) and the NSF-GRFP (N.X.G.), and the authors acknowledge the Dow Next Generation Educator Fund. We thank Dr. Michael Takase and Lawrence Henling for assistance with X-ray crystallography and Nathanael Hirscher for assistance with Toepler pump experiments.

Conflicts of interest

There are no conflicts to declare.

Notes and references

- ¹ (a) D. Sippel, O. Einsle, *Nat. Chem. Bio.* 2017, **13**, 956. (b) T. Spatzal, M. Aksoyoglu, L. Zhang, S. L. A. Andrade, E. Schleicher, S. Weber, D. C. Rees, O. Einsle *Science* 2011, **334**, 940.
- ² (a) R. R. Eady, *Chem. Rev.* 1996, **96**, 3013. (b) Y. Hu, M. W. Ribbe, *J. Biol. Inorg. Chem.* 2015, **20**, 435.
- ³ (a) D. Sippel, M. Rohde, J. Netzer, C. Trncik, J. Gies, K. Grunau, I. Djurdjevic, L. Decamps, S. L. A. Andrade, O. Einsle, *Science* 2018, **359**, 1484. (b) B. Benediktsson, A. T. Thorhallsson, R. Bjornsson. *Chem. Commun.* 2018, **54**, 7310.
- ⁴ Y. Sekiguchi, K. Arashiba, H. Tanaka, A. Eizawa, K. Nakajima, K. Yoshizawa, Y. Nishibayashi, *Angew. Chemie. Int. Ed.* 2018, **57**, 1.
- ⁵ (a) For representative examples see: J. S. Anderson, J. Rittle, J. C. Peters, *Nature* 2013, **501**, 84. (b) G. Ung, J. C. Peters, *Angew. Chemie. Int. Ed.* 2015, **54**, 532. (c) S. Kuriyama, K. Arashiba, K. Nakajima, Y. Matsuo, H. Tanaka, K. Ishii, K. Yoshizawa, Y. Nishibayashi, *Nat. Commun.* 2016, **7**, 12181. (d) P. J. Hill, L. R. Doyle, A. D. Crawford, W. K. Myers, A. E. Ashley, *J. Am. Chem. Soc.* 2016, **138**, 13521. (e) T. M. Buscagan, P. H. Oyala, J. C. Peters, *Angew. Chem. Int. Ed.* 2017, **56**, 6921. (f) S. E. Creutz, J. C. Peters, *J. Am. Chem. Soc.* 2014, **136**, 1105. (g) M. J. Chalkley, T. J. Del Castillo, B. D. Matson, J. P. Roddy, J. C. Peters, *ACS Cent. Sci.* 2017, **3**, 217. (h) M. J. Chalkley, T. J. Del Castillo, B. D. Matson, J. P. Roddy, J. C. Peters, *J. Am. Chem. Soc.* 2018, **140**, 6122.
- ⁶ (a) S. M. Malinak, K. D. Demadis, D. Coucouvanis, *J. Am. Chem. Soc.* 1995, **117**, 3126. (b) D. Coucouvanis, K. D. Demadis, S. M. Malinak, P. E. Mosier, M. A. Tyson, L. J. Laughlin, *J. Mol. Catal. A: Chem.* 1996, **107**, 123.
- ⁷ M. J. Dilworth, R. R. Eady, *Biochem. J.* 1991, **277**, 465.
- ⁸ L. C. Davis, *Arch. Biochem. Biophys.* 1980, **204**, 270.
- ⁹ (a) S. Kuwata, Y. Mizobe, M. Hidai, *Inorg. Chem.* 1994, **33**, 3619. (b) I. Takei, K. Dohki, K. Kobayashi, T. Suzuki, M. Hidai, *Inorg. Chem.* 2005, **44**, 3768. (c) K. Umehara, S. Kuwata, T. Ikariya, *J. Am. Chem. Soc.* 2013, **135**, 6754. (d) P. B. Hitchcock, D. L. Hughes, M. J. Maguire, K. Marjani, R. L. Richards, *J. Chem. Soc., Dalton Trans.* 1997, 4747 (e) B. Wu, K. M. Gramigna, M. W. Bezpalko, B. M. Foxman, C. M. Thomas, *Inorg. Chem.* 2015, **54**, 1090. (f) S. M. Malinak, D. Coucouvanis *Prog. Inorg. Chem.* 2001, **49**, 599. (g) Block, E.; Ofori-Okai, G.; Kang, H.; Zubieta, J. *J. Am. Chem. Soc.* 1992, **114**, 758. (h) Under photolysis, $[\text{Mo}(\text{CN})_8]^{4-}$ was demonstrated to catalyse N_2H_4 disproportionation with yields of $>10^3$ equivalents of NH_3 . See: J. Szkiarzewicz, D. Matoga, A. Klyś, W. Łasocha, *Inorg. Chem.* 2008, **47**, 5464. (i) Saouma, C. T.; Moore, C. E.; Rheingold, A. L.; Peters, J. C. *Inorg. Chem.* 2011, **50**, 11285.
- ¹⁰ S. E. Creutz, J. C. Peters, *J. Am. Chem. Soc.* 2015, **137**, 7310.
- ¹¹ N. P. Mankad, M. T. Whited, J. C. Peters, *Angew. Chem. Int. Ed.* 2007, **46**, 5768.
- ¹² (a) Y.-H. Chang, C.-L. Su, R.-R. Wu, J.-H. Liao, Y.-H. Liu, H.-F. Hsu, *J. Am. Chem. Soc.* 2011, **133**, 5708. (b) H.-F. Hsu, W.-C. Chu, C.-H. Hung, J.-H. Liao, *Inorg. Chem.* 2003, **42**, 7369. (c) S. Ye, F. Neese, A. Ozarowski, D. Smirnov, J. Krzystek, J. Telsler, J.-H. Liao, C.-H. Hung, W.-C. Chu, Y.-F. Tsai, R.-C. Wang, K.-Y. Chen, H.-F. Hsu, *Inorg. Chem.* 2010, **49**, 977. (d) W.-C. Chu, C.-C. Wu, H.-F. Hsu, *Inorg. Chem.* 2006, **45**, 3164.
- ¹³ N. X. Gu, P. H. Oyala, J. C. Peters, *J. Am. Chem. Soc.* 2018, **140**, 6374.
- ¹⁴ A. Takaoka, N. P. Mankad, J. C. Peters, *J. Am. Chem. Soc.* 2011, **133**, 8440.
- ¹⁵ For reference, the Fe-H stretches of **9** and **10** are 1910 cm^{-1} and 1852 cm^{-1} , respectively.
- ¹⁶ Volatiles from a catalytic run performed in Et_2O were passed through a 77 K cold trap, and the remaining gas was quantified with a Toepler pump. The ammonia content from the same run was also determined. Representative IR data of catalyst mixtures after turnover do not reveal any Fe-N₂ stretches, indicating that the bound N₂ of **8** dissociates during catalysis (see Fig. S10 in the Supplementary Information). Omitting the equivalent of N₂ that is introduced into the headspace from **8**, a ratio of 4.0 NH₃ molecules per gas molecule is generated, consistent with the anticipated ratios for hydrazine disproportionation ($3\text{ N}_2\text{H}_4 \rightarrow 4\text{ NH}_3 + \text{N}_2$).
- ¹⁷ Carrying out entry C in the presence of elemental Hg or PPh₃ (0.3 equiv./**8**) demonstrated no significant attenuation of catalytic activity. (Hg: 46 equiv. NH₃/**8**; PPh₃: 42 equiv. NH₃/**8**)
- ¹⁸ C. Milsmann, S. P. Semproni, P. J. Chirik, *J. Am. Chem. Soc.* 2014, **136**, 12099.
- ¹⁹ The catalytic runs in Table 2 were performed in THF rather than Et_2O because of the poor solubility of **9** in Et_2O .
- ²⁰ Although complex **8** is a more active catalyst in Et_2O , the reaction order on N₂H₄ and **8** were determined in THF because it is miscible with hydrazine.
- ²¹ (a) H. R. Tang, D. M. Stanbury, *Inorg. Chem.* 1994, **33**, 1388. (b) E. Wiberg, N. Wiberg, *Inorganic Chemistry*; Academic Press: San Diego, CA, 2001. (c) N. Wiberg, H. Bachhuber, G. Fischer, *Angew. Chem. Int. Ed.* 1972, **11**, 829.



198x61mm (300 x 300 DPI)